Published in final edited form as:
Neuron. 2005 May 5; 46(3): 469–482. doi:10.1016/j.neuron.2005.03.027.

Long-Term Plasticity Mediated by mGluR1 at a Retinal Reciprocal Synapse

Jozsef Vigh, **Geng-Lin Li**, **Court Hull**, and **Henrique von Gersdorff***
The Vollum Institute, Oregon Health and Science University, 3181 S.W. Sam Jackson Park Road, Portland, Oregon 97239

Summary

The flow of information across the retina is controlled by reciprocal synapses between bipolar cell terminals and amacrine cells. However, the synaptic delays and properties of plasticity at these synapses are not known. Here we report that glutamate release from goldfish Mb-type bipolar cell terminals can trigger fast (delay of 2–3 ms) and transient $GABA_A$ IPSCs and a much slower and more sustained $GABA_C$ feedback. Synaptically released glutamate activated mGluR1 receptors on amacrine cells and, depending on the strength of presynaptic activity, potentiated subsequent feedback. This poststimulus enhancement of GABAergic feedback lasted for up to 10 min. This form of mGluR1-mediated long-term synaptic plasticity may provide retinal reciprocal synapses with adaptive capabilities.

Introduction

Retinal bipolar cells amplify and process the light/dark signals first detected by photoreceptors. They transmit these signals at the inner plexiform layer (IPL) via ribbon-type synapses onto ganglion cells, the output elements of the vertebrate retina, and onto amacrine cells. Thus, all visual information transferred from photoreceptors to the brain has to pass through the bottleneck filter of the bipolar cell presynaptic terminal in the IPL. Given this critical role, it is perhaps not surprising that the bipolar cell terminal receives a massive and elaborate input from one of the most diverse classes of inhibitory interneurons within the CNS, the amacrine cells (Masland, 2001). The importance of this inhibitory control is well demonstrated by serial EM reconstruction of the Mb-type bipolar cell terminal in goldfish: the terminal receives ≈350 distinct amacrine cell synapses (98% GABAergic, of which 59% are reciprocal), but makes only 60 excitatory contacts to ganglion cells (Marc and Liu, 2000), resulting in roughly six inhibitory (feedback) synapses per excitatory ganglion cell contact. Functionally, it has been suggested that inhibitory interactions at the bipolar cell terminal microcircuit may contribute to fundamental features of vision, such as sensitivity to light (Euler and Masland, 2000), temporal processing and motion (Cook and McReynolds, 1998; Roska et al., 1998), ganglion cell spike rate and receptive field size (Lukasiewicz et al., 2004), adaptation (Kim and Rieke, 2001; Baccus and Meister, 2002; Demb, 2002), and contrast detection (Jacobs and Werblin, 1998).

The large Mb bipolar cell terminal in goldfish retina allows voltage-clamped membrane current and capacitance measurements directly from the isolated presynaptic terminal in retinal slices (bipolar cell axon severed during slicing; Palmer et al., 2003b). It thus provides an ideal system for investigating the relationship between presynaptic Ca^{2+} influx, synaptic vesicle exocytosis of glutamate, and the subsequent reciprocal inhibitory input from

*Correspondence: vongersd@ohsu.edu.

amacrine cells. We find that exocytosis from the bipolar cell terminal triggers two events: a fast, transient inhibition of I_{Ca} mediated by proton release (DeVries, 2001; Palmer et al., 2003a) and a superimposed long-lasting GABAergic feedback. Here we show that the Ca^{2+} current inhibition can be blocked by intra-cellular methylamine without disrupting exocytosis (or glutamate release). An acidic vesicular pH is therefore not acutely needed for glutamate retention in synaptic vesicles. Intracellular methylamine allowed us to isolate the GABAergic feedback and thus study its delay and kinetics more precisely. Although GABAergic reciprocal feedback was observed previously in different species, its pharmacology and the mode of activation have remained controversial (Dong and Werblin, 1998; Protti and Llano, 1998; Hartveit, 1999; Shen and Slaughter, 2001; Singer and Diamond, 2003). In particular, its kinetics during the bipolar cell depolarization has not been studied directly from the terminal. Furthermore, synaptic plasticity at reciprocal synapses in the retina has not been explored.

We show here that evoked GABA released from amacrine cells activates both $GABA_A$ and $GABA_C$ receptors on the Mb bipolar cell terminal (Hull and von Gersdorff, 2004). In addition, we found that activation of mGluR1 localized to amacrine cells with DHPG, a group I mGluR agonist, greatly enhanced the reciprocal feedback. More importantly, mGluR1 receptors could be activated by synaptically released glutamate in an activity-dependent manner. However, this occurred only after bipolar cells were strongly depolarized or were depolarized for prolonged periods. Once mGluR1 was activated, it boosted the reciprocal feedback by enhancing GABA release from amacrine cells. We thus propose that after prolonged stimulation reciprocal synapses in the retina can undergo a form of mGluR1-mediated long-term plasticity that lasts for several minutes.

Results

Proton- and GABA-Mediated Inhibitory Feedback

Depolarization of Mb-type bipolar cell terminals in the goldfish retinal slice from a holding potential of −60 mV to 0 mV activated an L-type Ca^{2+} current (I_{Ca}; Heidel-berger and Matthews, 1992), which peaked within 1.0 ± 0.1 ms (n = 13). The amplitude ranged between 180 and 515 pA and averaged 362 ± 87 pA, while the resting membrane capacitance (C_m) averaged 6.1 ± 1.4 pF (n = 13). Thus, the average peak current density was 59 ± 10 pA/pF. A 200 ms step to 0 mV also triggered exocytosis, as reflected by the jump in membrane capacitance (ΔC_m = 250 ± 70 fF; n = 13). The “exocytotic index” ($\Delta C_m/restC_m \times 100$) thus averaged 4.0 ± 0.8 (n = 13), which means that a 200 ms step to 0 mV triggered a 4% increase in the membrane surface area of the bipolar cell terminal. Depolarization of the terminal evoked a flurry of outward synaptic currents overlaying I_{Ca} (Figure 1Ai, black trace; E_{Cl} = −41 mV). The magnitude of these feedback currents varied from terminal to terminal and was roughly correlated with the recorded bipolar cell terminal’s depth in the slice: deeper terminals had larger feedback, consistent with having more intact synaptic clefts and attached boutons. We usually recorded from terminals that were 10–40 μm deep in the 200–250 μm thick slices. Application of picrotoxin (PTX; 100 μM), which blocks both ionotropic GABA (A and C) receptors (Feigenspan et al., 1993), completely abolished the evoked feedback (Figure 1Ai, red trace), suggesting that it was mediated by inhibitory amacrine cells. After the Cl^- influx block, note the decrease in the Ca^{2+}-dependent Cl^- channel-mediated tail current ($I_{Cl(Ca)}$; Figure 1Ai, arrow), which depends on both the $[Ca^{2+}]i$ and $[Cl^-]_i$ in bipolar cells (Okada et al., 1995; Hull and von Gersdorff, 2004). Experiments with strychnine (up to 8 μM; a glycine receptor antagonist) in the bath did not block any portion of the inhibitory feedback, indicating that it was purely GABAergic (n = 7; data not shown). The picrotoxin-insensitive initial portion of the feedback was always eliminated by switching to a 48 mM HEPES-based Ringer (Figure 1Aii inset, blue trace; n =

6), as shown previously in Mb bipolar cell terminals (Palmer et al., 2003a) and cones (DeVries, 2001).

Glutamate release from the terminal therefore initiated two distinct types of feedback: (1) a transient proton-mediated inhibition of I_{Ca} with a fast onset and (2) a longer-lasting inhibition, mediated by GABA. The proton-mediated feedback rose immediately from the peak of I_{Ca}, so its delay to onset could not be measured, and it peaked consistently within 1.3 ± 0.2 ms (n = 13; measured from the I_{Ca} peak). The earliest peak for the GABA-mediated feedback (marked with * on Figure 1Aii) had a short delay (2.8 ± 0.6 ms, n = 13; measured from the I_{Ca} peak) in the same cells, whereas its onset was hidden by the overlapping proton effect on I_{Ca}.

Buffering Vesicular Protons Coreleased with Glutamate

In order to isolate the GABAergic feedback, we sought ways to eliminate the pH-mediated effect on I_{Ca}. Though external HEPES (48 mM, Figures 1Ai and 1Aii) effectively blocked the pH-mediated feedback on I_{Ca}, we found that this high concentration of HEPES also greatly reduced the transmitter-mediated feedback and longevity of recordings, presumably due to the disruption of intracellular pH regulation under these conditions (Takahashi and Copenhagen, 1992). Therefore, we eliminated the pH gradient within synaptic vesicles before fusion by including methylamine, a weak base in the patch pipette (Johnson, 1987). With 10 mM methyl-amine in the pipette, the 200 ms depolarizations from −60 to 0 mV evoked I_{Ca} with amplitude between 245 and 390 pA that averaged 298 ± 45 pA and peaked at 1.1 ± 0.2 ms (n = 25). The same Mb bipolar cell terminals had 5.3 ± 1.5 pF resting C_m and a ΔC_m = 210 ± 64 pF. Thus, the “exocytotic index” was 3.9 ± 0.6. All of these values are almost identical to control measurements obtained in the absence of methylamine, suggesting that methylamine did not affect either the I_{Ca} or exocytosis. Furthermore, after <1 min of intracellular perfusion with methylamine, the pH effect on I_{Ca} was largely eliminated, but the depolarization of the bipolar cell terminal still evoked vigorous reciprocal GABAergic feedback (Figure 1Bi, black trace). The first evoked IPSC peaked at 3.4 ± 1.2 ms (marked with an asterisk on Figure 1Bii; n = 10) and all IPSCs were eliminated by PTX (Figure 1Bii, red trace; n = 5). In the presence of methylamine, the feedback was also blocked by the mixture of AMPA and NMDA antagonists (25 μM NBQX and 50 μM D-AP5; Figures 1Ci and 1Cii, red trace; n = 9; Dixon and Copenhagen, 1992; Hull and von Gersdorff, 2004). The presence of the GABAergic feedback indicates that amacrine cells were excited by glutamate release that persists despite an acute loss of the vesicular pH gradient (Cousin and Nicholls, 1997). Therefore, we routinely added methylamine to the patch pipette solution to isolate the GABAergic feedback onto the bipolar cell terminal in the experiments reported below.

Poststimulus Enhancement of the Reciprocal Feedback

During the first few minutes of repetitive 200 ms depolarizing pulses >35 s apart, reciprocal feedback responses showed no change if bipolar cell terminals were depolarized to −30 mV (up to three times, n = 6), but the GABA feedback was increased if we delivered a stronger depolarizations repeatedly to 0 mV (Figure 2Ai). Note that the red trace (second pulse to 0 mV) had significantly more feedback than the black trace (first pulse to 0 mV), in spite of the small rundown in ΔC_m. This suggests that GABA release has been potentiated. We called this enhancement of the feedback poststimulus enhancement (PSE). We quantified the increase between the consecutive depolarization-evoked feedback responses by simply measuring the decrease in the second depolarization-evoked I_{Ca} net charge transfer (integral of the evoked membrane current): $100 - [(Q_{Net(2nd)}/Q_{Net(1st)}) \times 100]$. We called this method of quantifying PSE the “ΔQ_{Net} method”. If the I_{Ca} peak amplitude rundown was ≥5% by the

second depolarization, terminals were excluded from evaluation to avoid artificial overestimation of the current charge Q_{Net} increase, even if they showed apparent PSE.

With pairs of 200 ms depolarizing pulses (from −60 to 0 mV) PSE for the reciprocal feedback evoked by the second depolarizing step was recorded in 25 terminals. The feedback increase (or enhancement) evaluated by the "ΔQ_{Net} method" averaged 15.4% ± 6.0% (range from 9% to 32%; n = 25, plotted on Figure 2Aii). The magnitude of this PSE did not depend on the interval between consecutive 200 ms long stimuli (Figure 2Aii), if it was at least 35 s in order to avoid paired-pulse depression (von Gersdorff and Matthews, 1997). We found only five bipolar terminals with no PSE in spite of the lack of rundown in their I_{Ca} and ΔC_m jump amplitude (data not shown). In numerous examples with no PSE (n > 30), quick and significant rundown of the I_{Ca} and/or C_m (>25%) occurred, and this could explain the lack of PSE.

Bipolar cell terminals that showed PSE sometimes still had a rundown of the depolarization-evoked exocytosis: the second depolarizing step was on average only 91% ± 11% (n = 25) of the first C_m jump. Consequently, our ΔQ_{Net} method probably systematically underestimated the degree of PSE. Therefore, we also quantified the amount of PSE with two other methods that utilized a double-pulse inhibition of exocytosis at the bipolar cell terminal (Palmer et al., 2003a). A typical recording is presented in Figure 2Bi. In these experiments, we applied two pairs of 100 ms depolarizations from −60 to 0 mV with a 350 ms interpulse interval, at least 1 min apart. To allow C_m measurements free of conductance changes, the amplitude of the $I_{Cl(Ca)}$ tail at −60 mV was reduced by decreasing the $[Cl^-]_i$ in the pipette to 11 mM (E_{Cl} = −56.7 mV). The first depolarizations (I_{1stA} and I_{2ndA}) evoked both I_{Ca} and ΔC_m, whereas the second depolarization (I_{1stB} and I_{2ndB}) evoked I_{Ca} of similar magnitude, yet little or no ΔC_m (Figure 2Bi). Glutamate was thus released only during the first step, so GABA feedback was triggered only then. Note the enhancement of feedback in the first step of the red trace when compared to the first step of the black trace.

Using the double-pulse protocol, I_{Cl} (the GABAergic Cl^- current) could be more precisely calculated ($I_{Cl1st} = I_{1stA} - I_{1stB}$ and $I_{Cl2nd} = I_{2ndA} - I_{2ndB}$, Figure 2Bii), as could Q_{Cl} (the integral of the I_{Cl} current; "ΔQ_{Cl} method"). Furthermore, we could account for the C_m rundown by normalizing Q_{Cl} to the ΔC_m ("$\Delta Q_{Cl}/\Delta C_m$ method"). A comparison of the different calculation methods (ΔQ_{Net} = 37.7% ± 22.2%; ΔQ_{Cl} = 63.9% ± 20.3%; and $\Delta Q_{Cl}/\Delta C_m$ = 55.5% ± 9.18%, n = 5) on the same cells revealed similar PSE magnitudes (Figure 2Biii). This analysis shows that the ΔQ_{Net} method tends to slightly underestimate the average amount of PSE when compared to either the ΔQ_{Cl} or $\Delta Q_{Cl}/\Delta C_m$ method. Nevertheless, the difference was not statistically significant ($p < 0.2$ for ΔQ_{Net} versus ΔQ_{Cl}, and $p < 0.1$ for ΔQ_{Net} versus $\Delta Q_{Cl}/\Delta C_m$, paired Student's t test). It is important to emphasize that in this set of experiments cells were excluded from evaluation if (1) the I_{Ca} peak amplitude rundown was ≥5% or (2) the double-pulse inhibition of exocytosis was not perfect (i.e., there was some feedback evoked by the second step of the pair); or (3) the rundown of the ΔC_m was more than 10%.

Group I mGluRs Located on Amacrine Cells Enhance the Reciprocal Feedback

Group I metabotropic glutamate receptors (mGluR1 and mGluR5) were detected using immuno-EM on amacrine cells postsynaptic to bipolar cell terminals in the rat retina (Koulen et al., 1997). Since their activation can either enhance or depress excitatory synapses (Snyder et al., 2001), we investigated the role of group I mGluRs in the reciprocal communication. Poststimulus enhancement (PSE) of the reciprocal feedback could be further enhanced by the selective group I mGluR agonist DHPG (50–100 μM) as demonstrated in Figure 3Ai (note that PSE occurs in spite of the rundown in ΔC_m). The average enhancement produced by DHPG ranged between 16% and 96% and averaged 42%

± 32% (ΔQ_{Net} method; n = 17), independent of the length of DHPG application used (Figure 3Aii). This suggests that mGluR1 activation might be involved in PSE.

We next wanted to determine the location of the DHPG-activated mGluRs influencing the reciprocal feedback. Group I mGluRs have been found both in the inner and outer retina: on amacrine cells postsynaptic to bipolar cell terminals in rat (Koulen et al., 1997), and on dendrites of certain bipolar cells (Koulen et al., 1997; Klooster et al., 2001). We first tested if DHPG acted in the inner or the outer retina of the goldfish when it enhanced the reciprocal feedback. In order to increase the average amplitude of the sIPSCs for some of these experiments, we doubled the $[Cl^-]_i$ in the pipette solution (E_{Cl} = −24 mV) to increase the driving force for Cl^- at our standard holding potential (−60 mV). Application of the AMPA/kainate receptor antagonist CNQX (25 μM) together with D-AP5 (50 μM) and TTX (1 μM) blocks the communication between bipolar cells and amacrine cells in the IPL as well as any spontaneous action potential spikes in amacrine cells. Under these conditions, the reciprocal feedback was eliminated (Figure 3Bi, red trace), and we observed a simultaneous decrease in both the number and the amplitude of the sIPSCs (Figures 3Bii–3Bv, red traces). After this pharmacological dissection of the inner retina, the addition of DHPG (100 μM) to the external Ringer produced a large increase in the sIPSC frequency and average amplitudes (Figures 3Bii–3Bv, blue traces), but this manipulation could not rescue the reciprocal feedback. Note the enhanced $I_{Ca(Cl)}$-mediated tail current, presumably due to the increased Cl^- influx via the sIPCSs (Figure 3Bi, blue trace). The DHPG-enhanced sIPSCs reversed polarity at the calculated E_{Cl} (data not shown). Adding $GABA_C$ and $GABA_A$ receptor blockers (TPMPA, 100 μM, and SR 95531, 25 μM, respectively) eliminated the sIPSCs (Figure 3Bii, green trace). The results were very consistent in all terminals tested (n = 8).

Although the increase of sIPSC frequency evoked by the DHPG strongly suggests an amacrine cell site of action, it was also possible that DHPG acted directly on the bipolar cell terminal. In cultured chick amacrine cells, for example, mGluR5 activation enhanced $GABA_A$ current amplitudes (Hoffpauir and Gleason, 2002), whereas group I mGluR agonists reduced the amplitude of the $GABA_C$ responses by 10%–30% in rat rod bipolar cells when tested with GABA puffs directly onto the bipolar cells in retinal slice (Euler and Wässle, 1998). We tested this possibility in two different ways. Acutely dissociated bipolar cell terminals were recorded in nystatin perforated-patch mode to prevent whole-cell dialysis in order to maintain the mGluR function (Euler and Wässle, 1998). We mimicked reciprocal feedback by puffing GABA onto the terminals during a 200 ms depolarizing step from −60 to 0 mV. Washing the cells with 100 μM DHPG for up to 4 min did not enhance the GABA-evoked current (Figure 4A) in any of the cells tested that responded to GABA (n = 7). DHPG (100 μM) also did not enhance GABA responses when we puffed GABA onto the Mb terminals during the same depolarizing steps in the retinal slice preparation in whole-cell recordings (n = 4, with 25 μM NBQX and 50 μM AP5 in the bath; data not shown).

Internal GDP-β-S blocks G protein-mediated group I mGluR activation evoked by DHPG (Tozzi et al., 2001). Nevertheless, when we included it in the pipette solution, GDP-β-S (1 mM; no GTP in the pipette solution) did not block the boosting effect of DHPG (100 μM) on the evoked reciprocal feedback (n = 5), even after several minutes of intracellular perfusion of the recorded bipolar cell terminals in slices (Figure 4B). This set of results thus strongly suggests that DHPG acted on amacrine cells in the inner retina to enhance the reciprocal feedback to the bipolar cell terminals.

$GABA_A$ and $GABA_C$ Receptors Mediate Feedback

We next tested whether the reciprocal feedback was mediated by distinct GABA receptors, and whether those were unevenly affected by the group I mGluR action. TPMPA (50–100 μM), a specific $GABA_C$ receptor antagonist (Ragozzino et al., 1996), reduced the reciprocal

feedback, particularly the late-occurring events (Figure 5Ai, red trace). The TPMPA-insensitive portion of the reciprocal feedback still had a very fast initial peak (with a peak delay of 3.5 ± 0.7 ms, n = 14) followed by a more complex and rather variable portion. $GABA_C$ receptors thus contribute to a significant part of the feedback. Application of the specific $GABA_A$ receptor antagonist bicuculline or SR 95531 (25 μM each, n = 8 and 13, respectively) revealed that the $GABA_C$ portion of the reciprocal feedback (Figure 5Aii, red trace) was different from that of $GABA_A$ in several aspects. First, it appeared to be much less spiky than the $GABA_A$ events, and its rise to peak took much longer: 76.7 ± 23.2 ms (n = 21; bicuculline and SR 95531 data pooled). In addition, $GABA_A$ block increased the leak current by 9.0 ± 4.5 pA (4 out of 4 terminals with bicuculline and 12 out of 13 terminals with SR 95531) at −60 mV holding potential, and this increase in leak was blocked by TPMPA (Figure 5Bii). This suggests that amacrine cells providing feedback to the bipolar cells receive inhibition from other amacrine cells via $GABA_A$ receptors, and blocking this connection disinhibits them, revealing a stronger tonic $GABA_C$ input to the bipolar cell terminal.

mGluR1 Action Boosts $GABA_A$ and $GABA_C$ Receptor-Mediated Feedback

Application of DHPG (50–100 μM) enhanced both the $GABA_A$ (n = 10 with TPMPA, Figure 5Ai, blue trace) and the $GABA_C$ (n = 8 with bicuculline and n = 4 with SR 95531, Figure 5Aii, blue trace) receptor-mediated reciprocal feedback. In all cases, the mGluR-boosted reciprocal feedback was completely blocked once both the $GABA_A$ and $GABA_C$ antagonists were present in addition to DHPG (Figures 5Ai and 5Aii, green traces). DHPG application further increased the leak current by about 10 pA after $GABA_A$ block, and this leak current was eliminated by subsequent TPMPA treatment (figure 5Bii). Accordingly, exposure to TPMPA prior to DHPG prevented the change in the leak (Figure 5Bi), suggesting that this leak current was associated with the high-affinity $GABA_C$ receptor activation.

Both members of group I mGluRs (1 and 5; Fagni et al., 2000) can be found on amacrine cell processes postsynaptic to bipolar cell ribbons in the rat (Koulen et al., 1997), and the DHPG at the concentrations that we used (50–100 μM) could equally activate them (Palmer et al., 1997). However, the effect of DHPG (100 μM) on the GABA evoked feedback could be prevented by coapplication of 50 μM LY367385 (n = 7, data not shown), a compound that selectively and reversibly blocks mGluR1 at this concentration (IC_{50} = 8.8 μM at mGluR1 and IC_{50} > 200 μM at mGluR5; Bruno et al., 1999). High concentrations (10–30 μM) of the highly specific mGluR5 blocker MPEP (IC_{50} = 36 nM, Gasparini et al., 1999) did not block the DHPG-mediated enhancement of the total feedback (n = 2, data not shown). Accordingly, we found that the specific mGluR5 agonist CHPG (500 μM to 1 mM; Doherty et al., 1997) was ineffective in boosting either component of the reciprocal feedback (n = 5 for $GABA_A$, Figure 5Ci; and n = 5 for $GABA_C$, Figure 5Cii). These results thus suggest the sole involvement of mGluR1, but not mGluR5 receptors, in enhancing the reciprocal feedback at the Mb bipolar cell terminal.

mGluR1 Mediates an Endogenous Poststimulus Enhancement of Feedback

The mGluR1 antagonist LY367385 (100 μM) reversibly blocked the PSE, once it was induced (n = 7; Figure 6Ai), in all seven terminals that were tested. In a separate set of experiments, cells were bathed in LY 367385 before the first depolarizing pulse to 0 mV. Under these circumstances, no PSE was recorded (5 out of 5 terminals); however, it took place when the mGluR1 antagonist was quickly washed out from the slices (2 out of 5; Figure 6Aii). These results thus suggested that synaptically released Glu activates mGluR1 on amacrine cell boutons, and their activity in turn mediates the PSE plasticity of the reciprocal feedback. However, the endogenous glutamate released by the depolarization of a

single bipolar terminal may not activate all the mGluR1 receptors located on reciprocally connected amacrine cells; therefore, only a fraction of the potentiating capacity was quenched this way. Addition of DHPG at high concentration will activate most (if not all) of them, so it can further increase the reciprocal feedback (compare red and blue traces on Figure 3Ai). In keeping with these results, the continuous presence of DHPG (100 μM) occluded the PSE evoked by synaptically released glutamate in every cell tested (n = 6; Figures 6Bi and 6Bii, gray bar). Figure 6Bii summarizes the magnitude of PSE (calculated by the ΔQ_{Net} method), depending on the DHPG presence.

Reciprocal Feedback Enhancement at More Physiological Membrane Potentials

Post stimulus enhancement of the reciprocal feedback at the bipolar cell terminal did not take place during depolarizations to −30 or −25 mV for 200 ms, but did occur when the same terminals were depolarized to 0 mV. This is a much stronger depolarization than the Mb terminals may experience under physiological conditions in response to light, when the membrane potential of the ON-type, Mb bipolar cell can reach about −20 mV (Saito and Kujiraoka, 1982; Protti et al., 2000) from the dark resting level of about −53 mV (Wong et al., 2005). We thus asked whether PSE of the reciprocal feedback takes place at more physiological membrane potentials. Therefore, we revisited the PSE using 200 ms pulses to −20 mV. Indeed, we observed a smaller enhancement of the feedback using a double-pulse paradigm: only three out of nine terminals showed marginal increase (3.9% ± 1.9%, n = 3). However, long depolarizations can occur in Mb-type bipolar cells in response to light. Therefore, in the next set of experiments we applied a 3 s “conditioning” step to −20 mV, between two 100 ms long test pulses to −20 mV (Figure 7Ai). Under these conditions, the second test pulse evoked larger feedback in six out of nine terminals. The increase in the feedback in these six cells ranged between 3.8% and 22.3%, averaged 8.8% ± 6.5% ($p < 0.04$ for two-tailed paired Student’s t test), and lasted for up to 10 min (Figure 7Aii). Note also that this PSE occurred in spite of the typical rundown in ΔC_m jumps during whole-cell recordings. We thus conclude that PSE can be induced by depolarizations to less positive (i.e., more physiological) membrane potentials, which reduce the presynaptic I_{Ca} amplitude, but under these conditions it requires longer stimuli.

Discussion

Our in situ presynaptic Ca^{2+} current and ΔC_m measurements revealed the extent of glutamate release from bipolar cell terminals and the timing and kinetics of the resulting reciprocal feedback from amacrine cells. Pharmacological manipulations dissected the magnitude and timing of $GABA_A$ and $GABA_C$ IPSCs. We report here a form of slowly activating synaptic plasticity in a reciprocal synapse of the retina that is mediated by mGluR1. We show that mGlu1 receptors are activated by synaptically released glutamate and that they are involved in a poststimulus enhancement of GABA release from amacrine cells. Our data suggest that the gain of a bipolar cell/amacrine cell reciprocal synapse is adjusted through an mGluR1-dependent synaptic mechanism.

The Timing of Inhibition at Bipolar Cell Terminals

The fastest inhibitory event at the Mb bipolar cell terminal was the proton-mediated inhibition of the Ca^{2+} current, with a consistent sharp peak at ≈1.3 ms (Palmer et al., 2003a), followed by a $GABA_A$ current-evoked peak at ≈2.8 ms (for 0 mV pulses; this delay was similar for −20 mV pulses, Figure 7Aii). The third, slowest peak of inhibition occurred at approximately 76 ms, was $GABA_C$ receptor dependent, and had a large jitter or variability in its peak. The GABAergic components could be isolated only after eliminating the effect of the synaptic cleft acidification on the Ca^{2+} current by intracellular methylamine perfusion. Although it has been suggested that methylamine does not decrease glutamate release from

synaptosomes (Cousin and Nicholls, 1997), our experiments demonstrate this by electrophysiological methods in a slice preparation. This question of whether ΔpH and/or ΔΨ(the vesicular membrane potential) are necessary for glutamate refilling of synaptic vesicles is controversial (Tabb et al. 1992). Our findings suggest that the activity of the vesicular glutamate transporter subtype detected in bipolar cell terminals, VGLUT1 (Fyk-Kolodziej et al., 2004), is dependent primarily on ΔΨ rather than on ΔpH. We conclude that dissipating the vesicular ΔpH with methylamine (1) did not eliminate the glutamate content of synaptic vesicles, and (2) it did not disrupt their exocytosis. By eliminating the pH effect on the Ca^{2+} current, we isolated the GABA receptor-mediated components of the feedback and uncovered their onset and kinetics.

$GABA_A$ and $GABA_C$ Reciprocal Feedback at the Bipolar Cell Terminal

Reciprocal feedback in salamander bipolar cells is primarily mediated by $GABA_C$ (Dong and Werblin, 1998), but in rat rod bipolar cells, Hartveit (1999) reported a contribution of both $GABA_A$ and $GABA_C$ receptors, whereas Singer and Diamond (2003) detected a $GABA_C$ portion in the reciprocal feedback only in the presence of cyclothiazide to enhance AMPA receptor activation and GABA spillover. Presynaptic $GABA_C$ receptors greatly modulate light responses of mouse rod bipolar cells (Lukasiewicz et al., 2004), and they are involved in limiting glutamate spillover on ON-transient amacrine cells (Matsui et al., 2001) and in the synchronization of quantal release from bipolar cells (Freed et al., 2003). Here, we conclude that (1) glycine receptors do not play a role in the reciprocal feedback at the Mb bipolar cell terminal, since the mixture of TPMPA and bicuculline/SR95531 completely (and reversibly) blocked feedback and strychnine did not reduce the IPSCs, and (2) both $GABA_A$ and $GABA_C$ receptors are activated during reciprocal feedback. The slow kinetics of the $GABA_C$ component might be attributable to several, not mutually exclusive, factors. First, the single-channel conductance of $GABA_C$ receptors is considerably smaller than that of $GABA_A$ receptors (Feigenspan et al., 1993). Second, the slow activation kinetics of the $GABA_C$ receptors could play a role (Amin and Weiss, 1994). Third, $GABA_A$ receptors may be located in the immediate vicinity of the GABA release sites, whereas $GABA_C$ receptors may be further away and are thus activated by GABA spillover (Figure 8; Singer and Diamond, 2003). Interestingly, $GABA_A$ and $GABA_C$ receptors are not co-localized at amacrine to bipolar cell synapses, nor has an extrasynaptic location for $GABA_C$ receptors been revealed in the IPL (Koulen et al., 1998; Zhang et al., 2002). Fourth, GABA release might be particularly slow from amacrine cells making $GABA_C$ receptor-mediated synapses onto Mb terminals (Figure 8). Further experiments will be needed to decide between these mechanisms.

Immunohistochemistry has revealed that a majority of the inputs to GABAergic amacrine cells arises from other GABAergic amacrine cells (Figure 8) in a variety of species (Zhang et al., 1997), including the goldfish (Marc and Liu, 2000). Therefore, in our experiments, $GABA_A$ blockers not only dissected the $GABA_C$ receptor-mediated reciprocal feedback, but they also disinhibited some of those amacrine cells synapsing on the recorded bipolar cell terminal and increased their GABA output (Watanabe et al., 2000; Zhang et al., 1997). We detected this by recording in the bipolar cell terminals a small increase in $GABA_C$ receptor-mediated reciprocal feedback (compare red traces and black traces on Figures 5Aii and 5Cii) and leak current increase (Figure 5Bii). $GABA_C$ receptors are particularly appropriate for contributing to such a “leak current” since they (1) are more sensitive than $GABA_A$ receptors (i.e., they have a higher affinity for GABA), (2) deactivate about eight times more slowly than $GABA_A$ receptors after agonist removal, and (3) show very little desensitization (Amin and Weiss, 1994).

Synaptic Plasticity in the Retina: mGluR1 Boosts the Reciprocal Feedback

Activation of mGluR1 is functionally coupled to phospholipase C, which generates IP_3 that in turn elevates $[Ca^{2+}]_i$ by releasing Ca^{2+} from intracellular compartments (Fagni et al., 2000). This mGluR1-triggered $[Ca^{2+}]_i$ increase has been implicated in various neuromodulatory processes, many of them leading to long-term changes in synaptic function in various CNS areas (Aiba et al., 1994; Lapointe et al., 2004). In the rat retina, mGluR1 was localized to amacrine cell processes postsynaptic to bipolar cell ribbons (Koulen et al., 1997). In fish retina, immunohistochemical investigations found mGluR1α-IR on bipolar cell dendrites (Klooster et al., 2001) and on wide-field amacrine cells (Vigh and Lasater, 2003). Ca^{2+} imaging studies of amacrine cell boutons have shown that they may act as local processing units independent of the activity in the cell soma (Euler et al., 2002), and some of them possess Ca^{2+} stores activated by mGluRs (Kreimborg et al., 2001). In keeping with these studies, in teleost GABAergic amacrine cells, the activation of mGluR1 decreased $GABA_A$ responses (Vigh and Lasater, 2003); therefore mGluR1s were suggested to provide an activity-dependent disinhibition of the amacrine cells close to an extremely active bipolar cell input, resulting in a stronger reciprocal feedback. Such a model mechanism is consistent with the present data (Figure 5). In addition, we suggest that mGluR1 activation increases the release probability of GABA release directly, probably through an elevation of intracellular $[Ca^{2+}]_i$ levels and/or a modification of the release machinery.

Here we have also shown that mGluR1 activation by DHPG is not sufficient to evoke reciprocal feedback by itself if the ionotropic AMPA and NMDA receptors are blocked (Figure 3Bi), although it enhances spontaneous transmitter release. Moreover, the DHPG-induced enhancement of the reciprocal feedback outlasted the increase in the spontaneous amacrine cell activity during the wash. In fact, we could never recover the control reciprocal feedback following a DHPG treatment, with-out an intervening rundown of I_{Ca} and/or ΔC_m jump in the terminal, whereas the DHPG effect on the spontaneous activity was reversible. Different mechanisms may therefore operate during DHPG enhancement of PSE and sIPSCs. We thus suggest that mGluR1 activation triggered long-lasting changes in the GABA release machinery of the amacrine cells in addition to an immediate boost of spontaneous activity.

Implications of Poststimulus Enhancement for Retinal Processing

What could be the physiological relevance for the retina of the poststimulus synaptic enhancement mechanism? Vision occurs over a wide range of contrast intensities, and one of the retina's basic challenges is to keep the excitatory inputs to ganglion cells in their dynamic range, in order to process small signals with sufficient gain and large signals without distortion due to saturation (Demb, 2002). There are compelling reports on intrinsic contrast adaptational mechanisms in both bipolar (Rieke, 2001) and ganglion cells (Kim and Rieke, 2001; Zaghloul et al., 2005) that occur within 100s of milliseconds to 10s of seconds. On the other hand, dopamine-dependent light adaptation processes work on a much longer time scale (Witkovsky, 2004). Some types of adaptation to contrast do not depend on inhibition (Rieke, 2001), whereas others may (Demb, 2002; Baccus and Meister, 2002). Finally, some "network adaptation" processes are characterized by increased inhibition (Cook et al., 2000). Clearly, the retina uses multiple mechanisms on different time scales to complete the task of adaptation.

Activation of feedback synapses onto the bipolar cell terminal has been shown to reduce glutamate release to ganglion cells by up to 28-fold (Pang et al., 2002). Such a robust inhibition is powered by the high gain at the bipolar cell to amacrine cell synapse (Copenhagen, 2004; Yang et al., 2002). Here we are showing that the GABAergic reciprocal inhibition of the bipolar cell terminal can be very strong, even in retinal slices, where a large

portion of the amacrine cell inputs may be lost. In addition, we observed an increase (up to 22%) in the feedback with more physiological membrane potential changes, due to an activity-dependent, long-lasting form of plasticity.

Could this relatively modest increase in the reciprocal feedback be physiologically relevant? First, we may be underestimating the magnitude of the in vivo mGluR1-mediated plasticity, due to the limitations of our preparation: whole-cell dialysis often causes a rundown in exocytosis, and the slicing procedure may decrease the total amacrine cell input. In addition, the integrity of the synaptic cleft around the recorded bipolar cell terminal may be reduced. Postsynaptic mGluR1s are perisynaptic in the hippocampus (Lujan et al., 1996). Since in the present set of experiments we needed strong presynaptic stimuli to activate mGluR1s, it is tempting to speculate that they are activated only by excess glutamate, perhaps at perisynaptic sites on the amacrine cells (Koulen et al., 1997). If so, the integrity of the synaptic cleft would be crucial for the full potency of the mechanism. Second, the light-evoked voltage responses of the Mb ON-type bipolar cells can be sustained (Saito and Kujiraoka, 1982; Wong et al., 2005). Given that ribbon synapses are specialized for continuous exocytosis (Sterling and Matthews, 2005), even a small increase of the inhibitory feedback could markedly influence the glutamate release by shunting the input resistance of the bipolar cell terminal, thereby reducing its voltage responses. Such a gain reduction might avoid EPSC saturation, and thus may fine-tune the bipolar cell output to the dynamic firing range of ganglion cells.

In summary, we propose that a mGluR1-mediated potentiation of the reciprocal feedback participates in downscaling the output of very active ON-type bipolar cells. The response of ganglion cells to contrast in different ambient light levels may thus adapt on a slow time scale via a mGluR1-triggered change of GABAergic inhibition at bipolar cell terminals.

Experimental Procedures

Retinal Slice Preparation

Retinal slices (200–250 μm) were prepared from goldfish (*Carassius auratus*; 8–14 cm) as described previously (Palmer et al., 2003b). Slices were transferred to the recording chamber and perfused continuously (2–3 ml/min) with Ringer comprised of 100 mM NaCl, 2.5 mM KCl, 1.0 mM $MgCl_2$, 2.5 mM $CaCl_2$, 25 mM $NaHCO_3$, and 12 mM glucose, at a pH of 7.45 (set with NaOH). The Ringer was gassed continuously with 95% O_2 and 5% CO_2. In experiments requiring different (48 mM) HEPES concentrations, the amounts of NaCl and NaOH were adjusted to maintain osmolarity (260 mOsm). Slice preparation and recordings were performed at room temperature (21°C–23°C) in daylight conditions. Slices were viewed with broad-spectrum white-light DIC optics through a 40× water-immersion objective coupled to a 2× premagnification (Optovart; Zeiss) or 1.6× zoom tube (Axioskop; Zeiss) and a CCD camera (Hamamatsu, Tokyo, Japan). Bipolar cell terminals were identified by their size, shape, and position in the slice, as well as depolarization-evoked Ca^{2+} currents and capacitance responses. A subset of isolated terminals was obtained by severing the bipolar cell axon during the slicing procedure, and they were identified via their single-exponential capacitative current response to a short hyperpolarizing voltage step from −60 mV (see Palmer et al., 2003b). The Mb terminal baseline membrane capacitance was 3–7 pF. Only isolated terminals were used for this study.

Dissociated Bipolar Cell Terminal Preparation

Goldfish retinal bipolar cells were acutely isolated as described previously (Heidelberger and Matthews, 1992). Isolated bipolar cell terminals were identified by their size and shape, as well as depolarization-evoked Ca^{2+} currents and C_m jumps. Recordings were made in

extracellular Ringer comprised of 120 mM NaCl, 2.5 mM KCl, 1.0 mM $MgCl_2$, 2.5 mM $CaCl_2$, 10 mM HEPES, 12 mM glucose, adjusted to desired pH with NaOH, 260 mOsm. Perforated-patch recordings were made by means of nystatin, mixing 4 μl freshly made stock solution (5 mg nystatin in 80 μl DMSO) into 1 ml pipette solution.

Electrophysiology

Whole-cell voltage-clamp recordings were obtained using 7–11 MΩ patch pipettes pulled from thick-walled borosilicate glass (World Precision Instruments, Sarasota, FL) using either a Narishige (model PP-830) or a Sutter (model P-97) puller. Pipettes were coated with wax to reduce pipette capacitance and electrical noise and were filled with a solution comprised of 115 mM Cs-gluconate, 25 mM HEPES, 10 mM TEA-Cl, 3 mM Mg-ATP, 0.5 mM Na-GTP, and 0.5 mM EGTA, adjusted to pH 7.2 with CsOH, 257 mOsm. Cs gluconate was replaced with CsCl for high intracellular Cl^- recordings. When methylamine hydrochloride (10 mM) was added, the amounts of Cs gluconate and CsOH were adjusted accordingly to maintain pH and osmolarity. Cells with R_s > 30 MΩ (or leak current > 50 pA at a holding potential of −60 mV) were excluded from any further evaluation. Data acquisition was controlled by “Pulse” software (HEKA, Lambrecht, Germany), and signals were recorded via a double EPC-9 (HEKA) patch-clamp amplifier. Sampling rates and filter settings were 10 and 3 kHz, respectively. Capacitance measurements were performed by the “sine + DC” method, in which a 1 kHz sinusoidal voltage command (30 mV peak to peak) was added to the holding potential of −60 mV, and the resulting current was analyzed at two orthogonal phase angles by the EPC-9 lock-in amplifier (Gillis, 2000).

Drug Application

Drugs were bath applied in the perfusing medium. For experiments requiring brief application of GABA, a Picospritzer was used to apply pressure (9 psi for 100 ms) to the back of a patch pipette (≈5 MΩ) positioned above the slice within 20 μm of the terminal. The pipette contained standard extracellular solution plus 10 mM GABA. NBQX, CNQX, CHPG, DHPG, MPEP, LY367385, SR95531, and AP5 were obtained from Tocris (Bristol, UK). All other chemicals and salts were obtained from Sigma (St. Louis, MO).

Analysis

Offline analysis of the data was performed with “IgorPro” software (Wavemetrics, Lake Oswego, OR) and SigmaPlot (SPSS, Chicago, IL). The increase in membrane capacitance, Cm, evoked by membrane depolarization, was measured as Cm = Cm(response) − Cm(baseline), where Cm (baseline) was the average Cm value during the 100 ms before the depolarizing step, and Cm (response) was the average Cm value measured over 50 or 100 ms after the step, starting 350–400 ms after repolarization to allow time for all evoked conductances to have decayed. Spontaneous postsynaptic inhibitory currents were recorded with 100 kHz sampling rate and analyzed offline with “Mini Analysis Program” (Synaptosoft, Inc. Decatur, GA). Automatically detected events (n = 69800 total) were then inspected visually to discard apparent noise from the analysis. Histograms are made by the program, evaluating data recorded for at least 2 min in each drug condition for every cell (n = 8).

Acknowledgments

We thank Dr. Paul Witkovsky, New York University Medical Center, and Dr. Ko Matsui, Vollum Institute, for critically reading and commenting on the manuscript. This research was supported by HFSP and NIH-NEI grants.

References

Aiba A, Kano M, Chen C, Stanton ME, Fox GD, Herrup K, Zwingman TA, Tonegawa S. Deficient cerebellar long-term depression and impaired motor learning in mGluR1 mutant mice. Cell. 1994; 79:377–388. [PubMed: 7954803]

Amin J, Weiss DS. Homomeric rho 1 GABA channels: activation properties and domains. Receptors Channels. 1994; 2:227–236. [PubMed: 7874449]

Baccus SA, Meister M. Fast and slow contrast adaptation in retinal circuitry. Neuron. 2002; 36:909–919. [PubMed: 12467594]

Bruno V, Battaglia G, Kingston A, O'Neill MJ, Catania MV, Di Grezia R, Nicoletti F. Neuroprotective activity of the potent and selective mGlu1a metabotropic glutamate receptor antagonist, (+)-2-methyl-4 carboxyphenylglycine (LY367385): comparison with LY357366, a broader spectrum antagonist with equal affinity for mGlu1a and mGlu5 receptors. Neuropharmacology. 1999; 38:199–207. [PubMed: 10218860]

Cook PB, McReynolds JS. Lateral inhibition in the inner retina is important for spatial tuning of ganglion cells. Nat Neurosci. 1998; 1:714–719. [PubMed: 10196588]

Cook PB, Lukasiewicz PD, McReynolds JS. $GABA_C$ receptors control adaptive changes in a glycinergic inhibitory pathway in salamander retina. J Neurosci. 2000; 20:806–812. [PubMed: 10632610]

Copenhagen, DR. Excitation in retina: The flow, filtering, and molecules of visual signaling in the glutamatergic pathways from photoreceptors to ganglion cells. In: Chalupa, LM.; Werner, JS., editors. The Visual Neurosciences. Cambridge, MA: The MIT Press; 2004. p. 320-333.

Cousin MA, Nicholls DG. Synaptic vesicle recycling in cultured cerebellar granule cells: role of vesicular acidification and refilling. J Neurochem. 1997; 69:1927–1935. [PubMed: 9349537]

DeVries SH. Exocytosed protons feedback to suppress the Ca2+ current in mammalian cone photoreceptors. Neuron. 2001; 32:1107–1117. [PubMed: 11754841]

Demb JB. Multiple mechanisms for contrast adaptation in the retina. Neuron. 2002; 36:781–783. [PubMed: 12467580]

Dixon DB, Copenhagen DR. Two types of glutamate receptors differentially excite amacrine cells in the tiger salamander retina. J Physiol. 1992; 449:589–606. [PubMed: 1355793]

Doherty AJ, Palmer MJ, Henley JM, Collingridge GL, Jane DE. (RS)-2-chloro-5-hydroxyphenylglycine (CHPG) activates mGluR5, but not mGluR1, receptors expressed in CHO cells and potentiates NMDA responses in the hippocampus. Neuropharmacology. 1997; 36:265–267. [PubMed: 9144665]

Dong CJ, Werblin FS. Temporal contrast enhancement via $GABA_C$ feedback at bipolar terminals in the tiger salamander retina. J Neurophysiol. 1998; 79:2171–2180. [PubMed: 9535976]

Euler T, Masland RH. Light-evoked responses of bipolar cells in a mammalian retina. J Neurophysiol. 2000; 83:1817–1829. [PubMed: 10758094]

Euler T, Wässle H. Different contributions of $GABA_A$ and $GABA_C$ receptors to rod and cone bipolar cells in a rat retinal slice preparation. J Neurophysiol. 1998; 79:1384–1395. [PubMed: 9497419]

Euler T, Detwiler PB, Denk W. Directionally selective calcium signals in dendrites of starburst amacrine cells. Nature. 2002; 418:845–852. [PubMed: 12192402]

Fagni L, Chavis P, Ango F, Bockaert J. Complex interactions between mGluRs, intracellular Ca^{2+} stores, and ion channels in neurons. Trends Neurosci. 2000; 23:80–88. [PubMed: 10652549]

Feigenspan A, Wässle H, Bormann J. Pharmacology of GABA receptor Cl^- channels in rat retinal bipolar cells. Nature. 1993; 361:159–162. [PubMed: 7678450]

Freed MA, Smith RG, Sterling P. Timing of quantal release from the retinal bipolar terminal is regulated by a feedback circuit. Neuron. 2003; 38:89–101. [PubMed: 12691667]

Fyk-Kolodziej B, Dzhagaryan A, Qin P, Pourcho RG. Immunocytochemical localization of three vesicular glutamate transporters in the cat retina. J Comp Neurol. 2004; 475:518–530. [PubMed: 15236233]

Gasparini F, Lingenhohl K, Stoehr N, Flor PJ, Heinrich M, Vranesic I, Biollaz M, Allgeier H, Heckendorn R, Urwyler S, et al. 2-Methyl-6-(phenylethynyl)-pyridine (MPEP), a potent, selective

and systemically active mGlu5 receptor antagonist. Neuropharmacology. 1999; 38:1493–1503. [PubMed: 10530811]

Gillis KD. Admittance-based measurement of membrane capacitance using the EPC-9 patch-clamp amplifier. Pflugers Arch. 2000; 439:655–664. [PubMed: 10764227]

Hartveit E. Reciprocal synaptic interactions between rod bipolar cells and amacrine cells in the rat retina. J Neurophysiol. 1999; 81:2923–2936. [PubMed: 10368409]

Heidelberger R, Matthews G. Calcium influx and calcium current in single synaptic terminals of goldfish retinal bipolar neurons. J Physiol. 1992; 447:235–256. [PubMed: 1317429]

Hoffpauir BK, Gleason EL. Activation of mGluR5 modulates $GABA_A$ receptor function in retinal amacrine cells. J Neurophysiol. 2002; 88:1766–1776. [PubMed: 12364505]

Hull C, von Gersdorff H. Fast endocytosis is inhibited by GABA-mediated chloride influx at a presynaptic terminal. Neuron. 2004; 44:469–482. [PubMed: 15504327]

Jacobs AL, Werblin FS. Spatiotemporal patterns at the retinal output. J Neurophysiol. 1998; 80:447–451. [PubMed: 9658062]

Johnson RG Jr. Proton pumps and chemiosmotic coupling as a generalized mechanism for neurotransmitter and hormone transport. Ann N Y Acad Sci. 1987; 493:162–177. [PubMed: 2884918]

Kim KJ, Rieke F. Temporal contrast adaptation in the input and output signals of salamander retinal ganglion cells. J Neurosci. 2001; 21:287–299. [PubMed: 11150346]

Klooster J, Studholme KM, Yazulla S. Localization of the AMPA subunit GluR2 in the outer plexiform layer of goldfish retina. J Comp Neurol. 2001; 441:155–167. [PubMed: 11745642]

Koulen P, Kuhn R, Wässle H, Brandstatter JH. Group I metabotropic glutamate receptors mGluR1alpha and mGluR5a: localization in both synaptic layers of the rat retina. J Neurosci. 1997; 17:2200–2211. [PubMed: 9045744]

Koulen P, Brandstatter JH, Enz R, Bormann J, Wässle H. Synaptic clustering of $GABA_C$ receptor rho-subunits in the rat retina. Eur J Neurosci. 1998; 10:115–127. [PubMed: 9753119]

Kreimborg KM, Lester ML, Medler KF, Gleason EL. Group I metabotropic glutamate receptors are expressed in the chicken retina and by cultured retinal amacrine cells. J Neurochem. 2001; 77:452–465. [PubMed: 11299308]

Lapointe V, Morin F, Ratte S, Croce A, Conquet F, La-caille JC. Synapse-specific mGluR1-dependent long-term potentiation in interneurones regulates mouse hippocampal inhibition. J Physiol. 2004; 555:125–135. [PubMed: 14673190]

Lujan R, Nusser Z, Roberts JD, Shigemoto R, Somogyi P. Perisynaptic location of metabotropic glutamate receptors mGluR1 and mGluR5 on dendrites and dendritic spines in the rat hippocampus. Eur J Neurosci. 1996; 8:1488–1500. [PubMed: 8758956]

Lukasiewicz PD, Eggers ED, Sagdullaev BT, McCall MA. $GABA_C$ receptor-mediated inhibition in the retina. Vision Res. 2004; 44:3289–3296. [PubMed: 15535996]

Marc RE, Liu W. Fundamental GABAergic amacrine cell circuitries in the retina: nested feedback, concatenated inhibition, and axosomatic synapses. J Comp Neurol. 2000; 425:560–582. [PubMed: 10975880]

Masland RH. The fundamental plan of the retina. Nat Neurosci. 2001; 4:877–886. [PubMed: 11528418]

Matsui K, Hasegawa J, Tachibana M. Modulation of excitatory synaptic transmission by $GABA_C$ receptor-mediated feedback in the mouse inner retina. J Neurophysiol. 2001; 86:2285–2298. [PubMed: 11698519]

Okada T, Horiguchi H, Tachibana M. Ca^{2+}-dependent Cl^- current at the presynaptic terminals of goldfish retinal bipolar cells. Neurosci Res. 1995; 23:297–303. [PubMed: 8545078]

Palmer MJ, Irving AJ, Seabrook GR, Jane DE, Collingridge GL. The group I mGlu receptor agonist DHPG induces a novel form of LTD in the CA1 region of the hippocampus. Neuropharmacology. 1997; 36:1517–1532. [PubMed: 9517422]

Palmer MJ, Hull C, Vigh J, von Gersdorff H. Synaptic cleft acidification and modulation of short-term depression by exocytosed protons in retinal bipolar cells. J Neurosci. 2003a; 23:11332–11341. [PubMed: 14672997]

Palmer MJ, Taschenberger H, Hull C, Tremere L, von Gersdorff H. Synaptic activation of presynaptic glutamate transporter currents in nerve terminals. J Neurosci. 2003b; 23:4831–4841. [PubMed: 12832505]

Pang JJ, Gao F, Wu SM. Relative contributions of bipolar cell and amacrine cell inputs to light responses of ON, OFF and ON-OFF retinal ganglion cells. Vision Res. 2002; 42:19–27. [PubMed: 11804628]

Protti DA, Llano I. Calcium currents and calcium signaling in rod bipolar cells of rat retinal slices. J Neurosci. 1998; 18:3715–3724. [PubMed: 9570802]

Protti DA, Flores-Herr N, von Gersdorff H. Light evokes Ca2+ spikes in the axon terminal of a retinal bipolar cell. Neuron. 2000; 25:215–227. [PubMed: 10707985]

Ragozzino D, Woodward RM, Murata Y, Eusebi F, Overman LE, Miledi R. Design and in vitro pharmacology of a selective gamma-aminobutyric acidC receptor antagonist. Mol Pharmacol. 1996; 50:1024–1030. [PubMed: 8863850]

Rieke F. Temporal contrast adaptation in salamander bipolar cells. J Neurosci. 2001; 21:9445–9454. [PubMed: 11717378]

Roska B, Nemeth E, Werblin FS. Response to change is facilitated by a three-neuron disinhibitory pathway in the tiger salamander retina. J Neurosci. 1998; 18:3451–3459. [PubMed: 9547252]

Saito T, Kujiraoka T. Physiological and morphological identification of two types of on-center bipolar cells in the carp retina. J Comp Neurol. 1982; 205:161–170. [PubMed: 7076890]

Shen W, Slaughter MM. Multireceptor GABAergic regulation of synaptic communication in amphibian retina. J Physiol. 2001; 530:55–67. [PubMed: 11136858]

Singer JH, Diamond JS. Sustained Ca^{2+} entry elicits transient postsynaptic currents at a retinal ribbon synapse. J Neurosci. 2003; 23:10923–10933. [PubMed: 14645488]

Snyder EM, Philpot BD, Huber KM, Dong X, Fallon JR, Bear MF. Internalization of ionotropic glutamate receptors in response to mGluR activation. Nat Neurosci. 2001; 4:1079–1085. [PubMed: 11687813]

Sterling P, Matthews G. Structure and function of ribbon synapses. Trends Neurosci. 2005; 28:20–29. [PubMed: 15626493]

Tabb JS, Kish PE, Van Dyke R, Ueda T. Glutamate transport into synaptic vesicles. Roles of membrane potential, pH gradient, and intravesicular pH. J Biol Chem. 1992; 267:15412–15418. [PubMed: 1353494]

Takahashi K, Copenhagen DR. APB suppresses synaptic input to retinal horizontal cells in fish: a direct action on horizontal cells modulated by intracellular pH. J Neurophysiol. 1992; 67:1633–1642. [PubMed: 1352805]

Tozzi A, Guatteo E, Caputi L, Bernardi G, Mercuri NB. Group I mGluRs coupled to G proteins are regulated by tyrosine kinase in dopamine neurons of the rat midbrain. J Neurophysiol. 2001; 85:2490–2497. [PubMed: 11387395]

Vigh J, Lasater EM. Intracellular calcium release resulting from mGluR1 receptor activation modulates $GABA_A$ currents in wide-field retinal amacrine cells: a study with caffeine. Eur J Neurosci. 2003; 17:2237–2248. [PubMed: 12814357]

von Gersdorff H, Matthews G. Depletion and replenishment of vesicle pools at a ribbon-type synaptic terminal. J Neurosci. 1997; 17:1919–1927. [PubMed: 9045721]

Watanabe S, Koizumi A, Matsunaga S, Stocker JW, Kaneko A. GABA-mediated inhibition between amacrine cells in the goldfish retina. J Neurophysiol. 2000; 84:1826–1834. [PubMed: 11024075]

Witkovsky P. Dopamine and retinal function. Doc Ophthalmol. 2004; 108:17–40. [PubMed: 15104164]

Wong YK, Cohen ED, Dowling J. Retinal bipolar cell input mechanisms in Giant Danio. II Patch-clamp analysis of ON bipolar cells. J Neurophysiol. 2005; 93:94–107. [PubMed: 15229214]

Yang XL, Gao F, Wu SM. Non-linear, high-gain and sustained-to-transient signal transmission from rods to amacrine cells in dark-adapted retina of Ambystoma. J Physiol. 2002; 539:239–251. [PubMed: 11850516]

Zaghloul KA, Boahen K, Demb JB. Contrast adaptation in subthreshold and spiking responses of mammalian Y-type retinal ganglion cells. J Neurosci. 2005; 25:860–868. [PubMed: 15673666]

Zhang J, Jung CS, Slaughter MM. Serial inhibitory synapses in retina. Vis Neurosci. 1997; 14:553–563. [PubMed: 9194322]

Zhang J, Li W, Trexler EB, Massey SC. Confocal analysis of reciprocal feedback at rod bipolar terminals in the rabbit retina. J Neurosci. 2002; 22:10871–10882. [PubMed: 12486181]

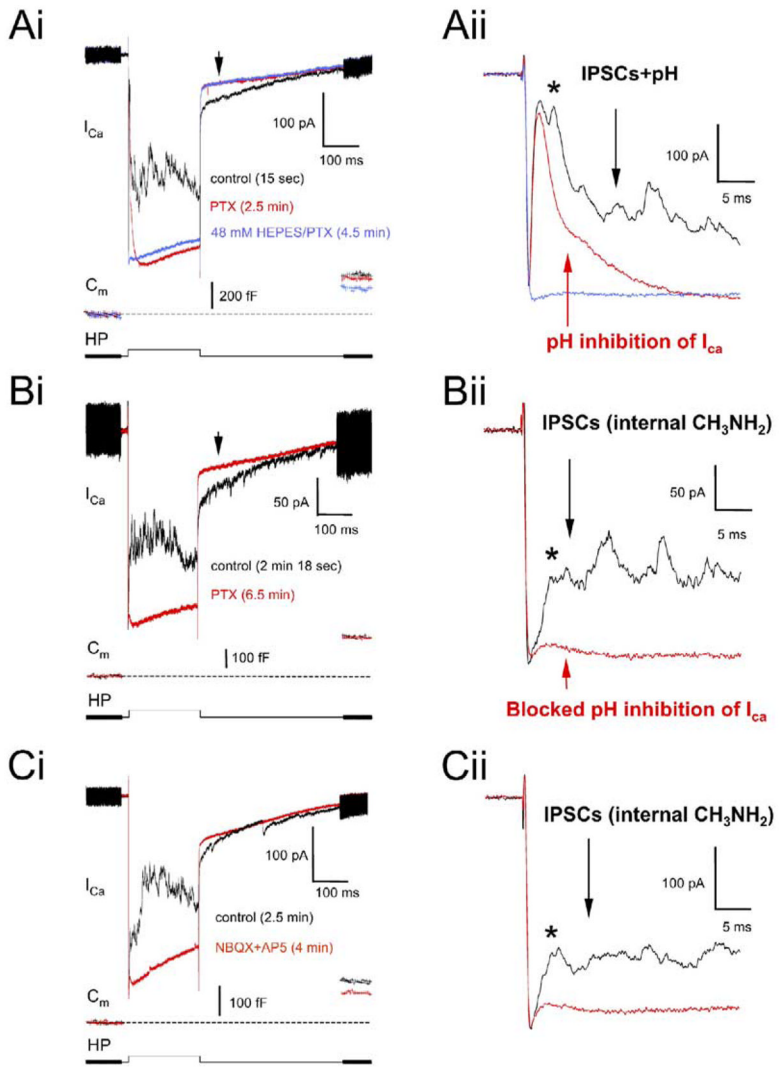

Figure 1. Depolarization of the Mb Bipolar Cell Terminal Evokes Two Types of Feedback

(Ai) Depolarization of the bipolar cell terminal from the holding potential of −60 mV to 0 mV for 200 ms activates Ca^{2+} influx through voltage-gated Ca^{2+} channels (I_{Ca}) that triggers exocytosis, as evidenced by the jump in the membrane capacitance (C_m). The inhibitory feedback to the presynaptic terminal is expressed as a flurry of outward inhibitory postsynaptic currents (IPSC) overlaying I_{Ca}. Picrotoxin (PTX; 100 μM) blocked the IPSCs and revealed the synaptic cleft acidification-dependent part (PTX, red trace; time is measured from break-in throughout the paper). This component is completely eliminated (see inset in [Aii]) when the extracellular Ringer contained 48 mM HEPES instead of the standard 25 mM bicarbonate. Note that exocytosis did not change in PTX (compare black and red C_m traces), but the Ca^{2+}-dependent Cl^- mediated tail current ($I_{Cl(Ca)}$, arrowhead) did after the elimination of Cl^- influx.

(Aii) Inset of (Ai). The first IPSC peak delay (asterisk) was 3.3 ms. Resting capacitance of this terminal was 6.1 pF.

(Bi) After 2 min and 18 s of intracellular perfusion with 10 mM methylamine (CH_3NH_2), the pH-mediated effect was largely blocked (see inset in [Bii]). Picrotoxin (100 μM) eliminated the IPSCs from amacrine cells (red trace). Note the unchanged exocytosis in PTX, but the change in the $I_{Cl(Ca)}$ (arrowhead).

(Bii) Inset of (Bi). The first IPSC peak delay (asterisk) was 2.7 ms. Resting capacitance was 4.0 pF.

(Ci) IPSCs were eliminated by the combination of ionotropic glutamate receptor antagonists NBQX and AP5 (25 and 50 μM, respectively), even though a ΔC_m jump was elicited in response to the 200 ms depolarization from −60 to 0 mV. Glutamate release thus needs to depolarize the amacrine cells for reciprocal GABA feedback. The patch pipette contained 10 mM methylamine.

(Cii) Inset of (Ci). The first IPSC peak delay (asterisk) was 3.0 ms. Resting capacitance was 4.0 pF.

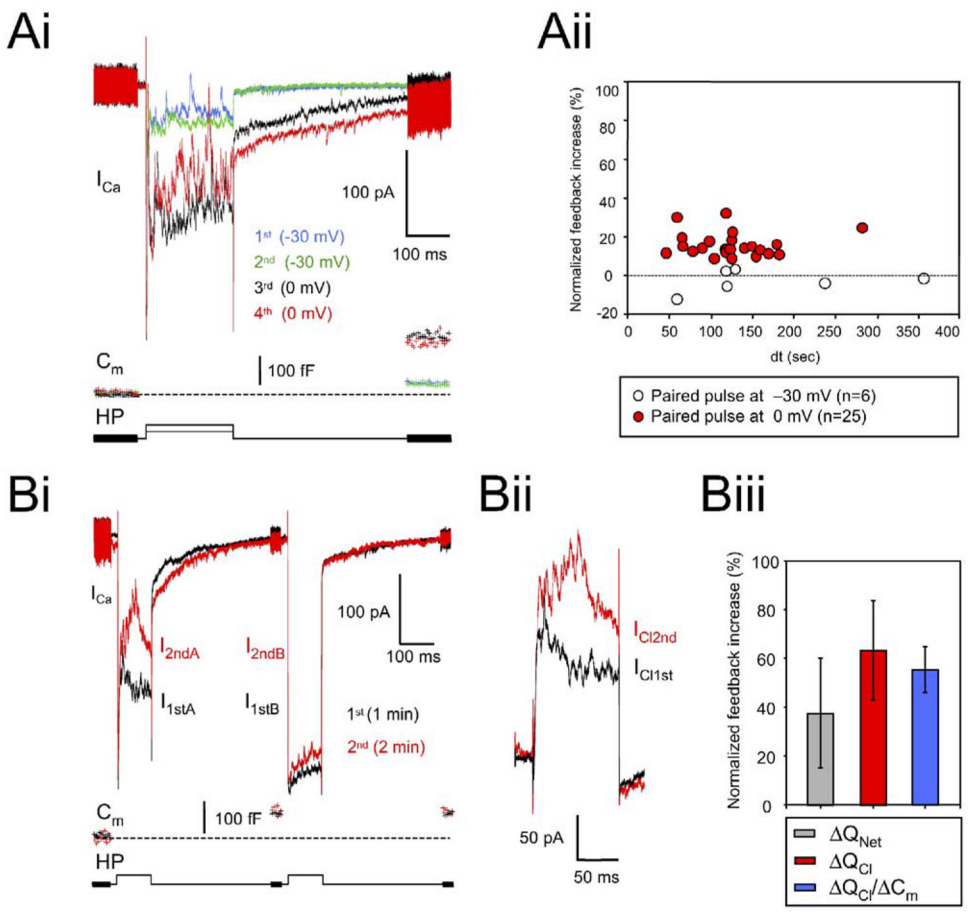

Figure 2. The Inhibitory Feedback during the Depolarization of the Bipolar Cell Terminal Is Evoked and Reciprocal and Shows Activity-Dependent Poststimulus Enhancement

(Ai) Repeated depolarizations to −30 mV evoked a small I_{Ca} and feedback (blue and green traces). However, if the same bipolar terminal was depolarized repeatedly to 0 mV afterward, an enhancement of the inhibitory feedback (IPSCs) was observed (compare black and red traces), even if the exocytosis was running down (compare black and red traces in the C_m). Note the corresponding increase in the $I_{Cl(Ca)}$ tail current as well, presumably reflecting the increase in Cl^- influx. The interval between consecutive steps was 2 min. The resting C_m of this terminal was 5.1 pF.

(Aii) Summary diagram of cells showing PSE. Increase in the feedback was measured by the normalized decrease of the I_{Ca} charge transfer (integral of the evoked membrane current) in response to a second depolarization (i.e., $100 - ((Q_{Net(2nd)}/Q_{Net(1st)}) \times 100)$, and plotted against the delay between the first and second stimuli. Cells included for the −30 mV pulses showed subsequent enhancement at 0 mV without exceptions.

(Bi) PSE quantification by using paired double pulses. Superimposed membrane currents (I_{Ca}) and ΔC_m evoked by two pairs of 100 ms voltage steps from −60 to 0 mV (350 ms apart). The pairs followed each other with 1 min delay. Glutamate release (ΔC_m jumps) was evoked only during the first pulse (I_{1stA} and I_{2ndA}) of the double pulses because bipolar cells exhibit strong paired-pulse depression. Consequently, only the I_{1stA} and I_{2ndA} steps triggered reciprocal GABA feedback. Accordingly, the $I_{Cl(Ca)}$ tail current is larger for the I_{1stA} and I_{2ndA} steps than for the second steps of the pulse pairs (I_{1stB} and I_{2ndB}, respectively). Note the large potentiation of the reciprocal feedback from I_{1stA} to I_{2ndA}. The resting C_m for this terminal was 4.1 pF.

(Bii) The total GABA feedback current (I_{Cl}) was calculated by subtracting the first I_{Ca} of the doubles showing feedback from the corresponding second, which showed none or little feedback ($I_{Cl1st} = I_{1stA} - I_{1stB}$ and $I_{Cl2nd} = I_{2ndA} - I_{2ndB}$ for the black and red traces, respectively).

(Biii) Comparison of different quantification methods for the PSE on the same set of cells (n = 5) revealed no significant difference among them. The different methods are $\Delta Q_{Net} = 100 - ((Q_{Net(2nd)}/Q_{Net(1st)}) \times 100)$ (gray bar), $\Delta Q_{Cl} = 100 - ((I_{Cl2nd}/I_{Cl1st}) \times 100)$ (red bar), and $\Delta Q_{Cl}/\Delta C_m = 100 - ((I_{Cl1st}/\Delta Cm_{lst})/(I_{Cl2nd}/\Delta Cm_{2nd}) \times 100)$ (blue bar).

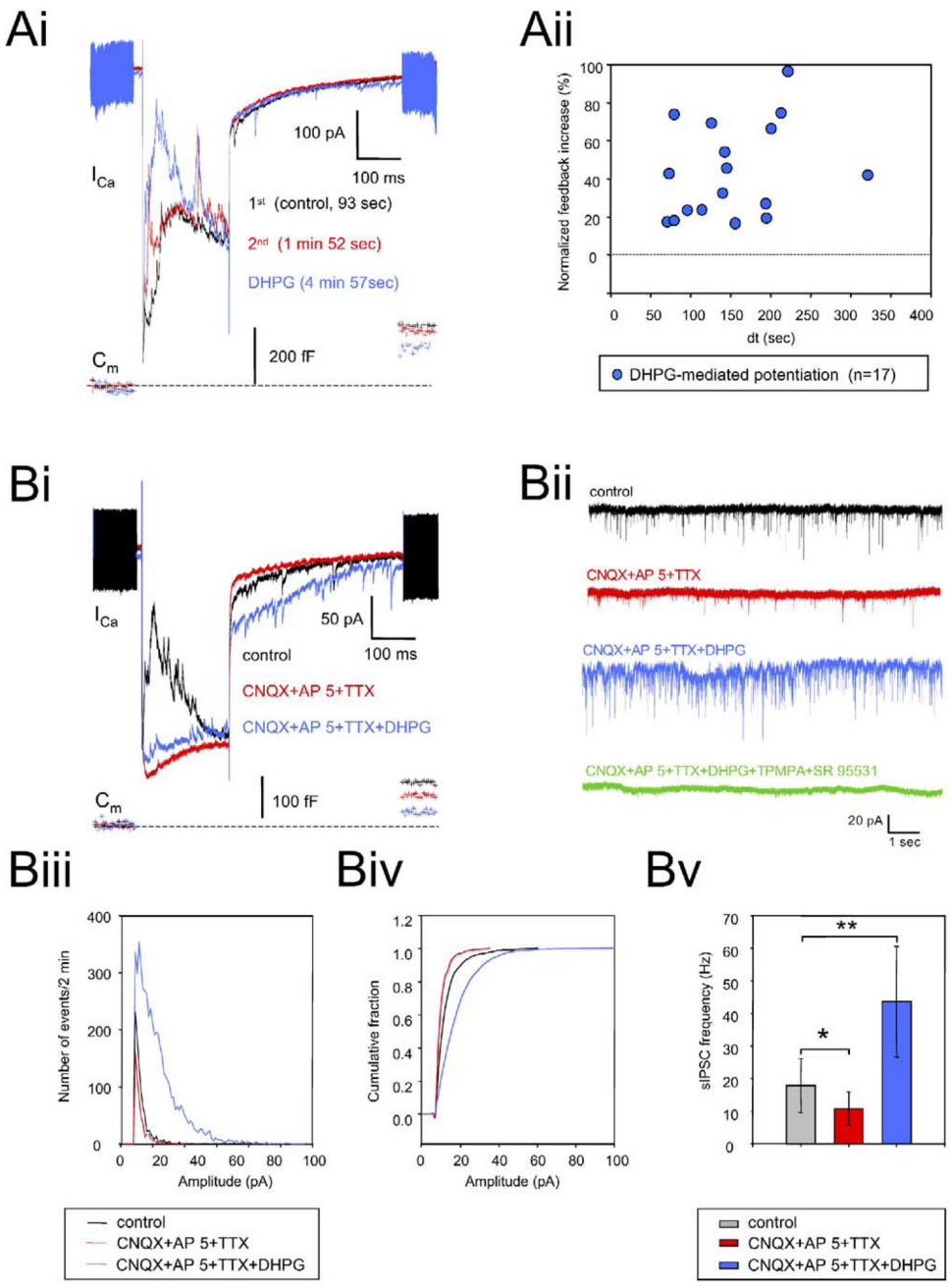

Figure 3. Group I mGluRs Located in the Inner Retina Are Involved in the PSE of the Reciprocal Feedback

(Ai) Poststimulus enhancement (PSE) of the reciprocal feedback (compare black and red traces) could be further enhanced by the group I mGluR agonist DHPG (50 μM, blue trace), even against the rundown of the exocytosis. The resting C_m of this terminal was 6.8 pF.

(Aii) Summary diagram of DHPG-mediated potentiation of the feedback, determined by the ΔQ_{Net} method. Data obtained with 50 and 100 μM DHPG were pooled, since the DHPG effect depended more on rundown of the bipolar cell terminal than the DHPG concentration. All terminals were depolarized from −60 to 0 mV.

(Bi) Application of the mixture of CNQX (25 μM) and AP 5 (50 μM) pharmacologically dissect the inner retina by blocking AMPA, KA, and NMDA receptors. TTX (1 μM) was

also added to block spontaneous action potentials in amacrine cells. Note that under these conditions the reciprocal feedback is completely eliminated (red trace). Including DHPG (100 μM) in the mixture did not recover the reciprocal feedback. The Ca^{2+}-dependent Cl^{-}-mediated tail current is markedly enhanced (blue trace), probably due to the higher Cl^{-} level in the terminal from the increased spontaneous inhibitory postsynaptic currents (sIPSCs).
(Bii) Corresponding sIPSC recordings from the same cell shown on (Bi). The cocktail of CNQX, AP5, and TTX reduced both the number and the size of the sIPSCs. Addition of DHPG on top of these blockers produced a robust increase in both the frequency and the amplitude of the sIPSCs.
(Biii) Amplitude frequency histogram analysis of the traces shown in (Bii). Bin size = 1.
(Biv) Cumulative fraction analysis of the sIPSCs represented in (Bii) revealed a small reduction in the size of the IPSCs in the mixture of CNQX, AP5, and TTX. The IPSC size was markedly increased when DHPG was added on top of CNQX, AP5, and TTX. Bin size = 1.
(Bv) Summary diagram of the sIPSC frequency changes exemplified in (Bii) (n = 8). *$p < 0.01$, **$p < 0.001$.

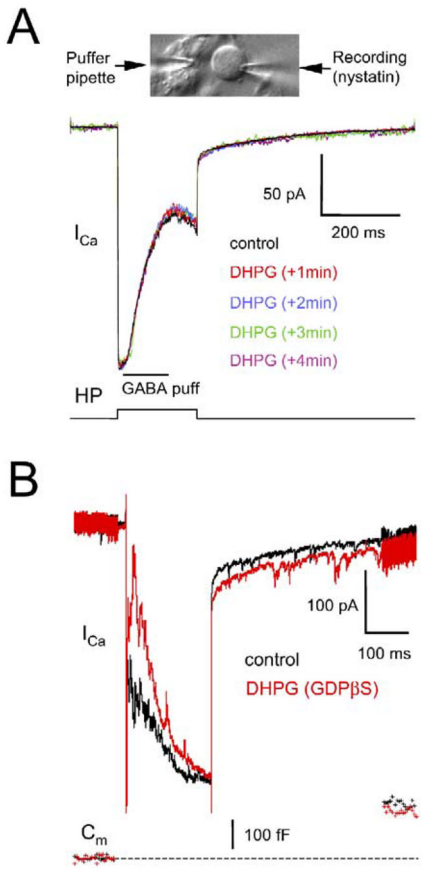

Figure 4. DHPG Did Not Alter GABA Receptor Function on the Bipolar Cell Terminals

(A) Reciprocal feedback was mimicked in isolated bipolar terminals recorded with the nystatin perforated-patch method by puffing GABA onto the terminals during a depolarization from −60 to 0 mV that evoked I_{Ca}. Application of DHPG (100 μM) for several minutes did not alter the GABA-evoked current.

(B) Including GDP-β-S (1 mM) in the patch pipette did not eliminate the DHPG-mediated enhancement of the feedback. The control trace (black) was taken at 2 min and 37 s after break-in. The DHPG trace (red) was recorded after an additional 3 min and 10 s. Thus, after 5 min and 47 s of intracellular perfusion with GDP-β-S, the feedback was still increased by DHPG. The resting C_m of this terminal was 4.5 pF.

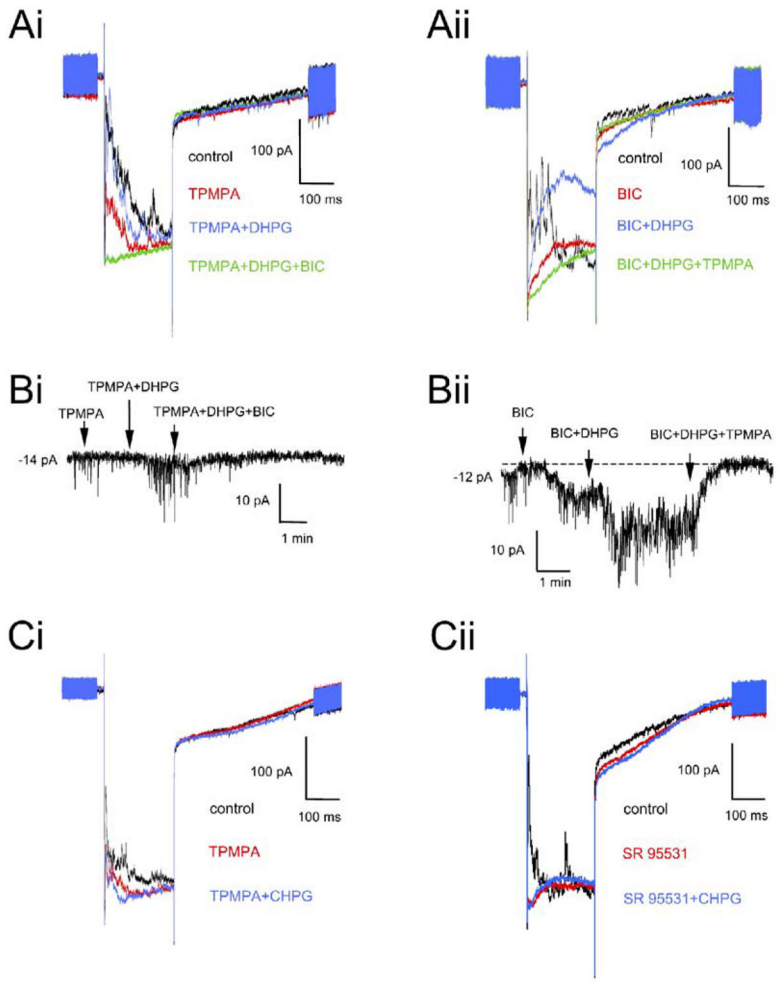

Figure 5. Pharmacology of the $GABA_{A/C}$ and Group I mGluRs Involved in the Enhancement of the Reciprocal Feedback

(Ai) After dissecting the $GABA_A$ portion of the reciprocal feedback with TPMPA (red trace), DHPG (100 μM) still enhanced the feedback (blue trace). Note that TPMPA and bicucul-line (50 μM and 25 μM, respectively) totally blocked the reciprocal feedback even in the presence of DHPG (green trace).

(Aii) When we dissected the $GABA_C$ portion of the reciprocal feedback first with bicucul-line (25 μM, red trace), the DHPG was still able to markedly enhance it (blue trace).

(Bi) $GABA_C$ block with TPMPA (100 μM) did not change the leak, neither did addition of DHPG (100 μM) in the presence of TPMPA. Nevertheless, the mGluR1 activation increased the baseline noise, which was eliminated by bicuculine (BIC, 25 μM), consistent with increased amacrine cell GABA output to $GABA_A$ receptors.

(Bii) Bicuculline (BIC, 25 μM) increased the leak current, which was further increased by DHPG (100 μM). The leak was eliminated upon addition of TPMPA (100 μM). This suggests that both agents (BIC and DHPG) increased the amacrine cell GABA output: BIC presumably by disinhibiting amacrine cells, and DHPG presumably via a $[Ca^{2+}]_i$ increase in amacrine cell synapses.

(Ci) The specific mGluR5 receptor agonist CHPG (1 mM) failed to enhance the $GABA_A$ receptor-mediated reciprocal feedback dissected with TPMPA.

(Cii) CHPG (1 mM) did not enhance the $GABA_C$ portion of the reciprocal feedback dissected with SR 95531 (25 μM).

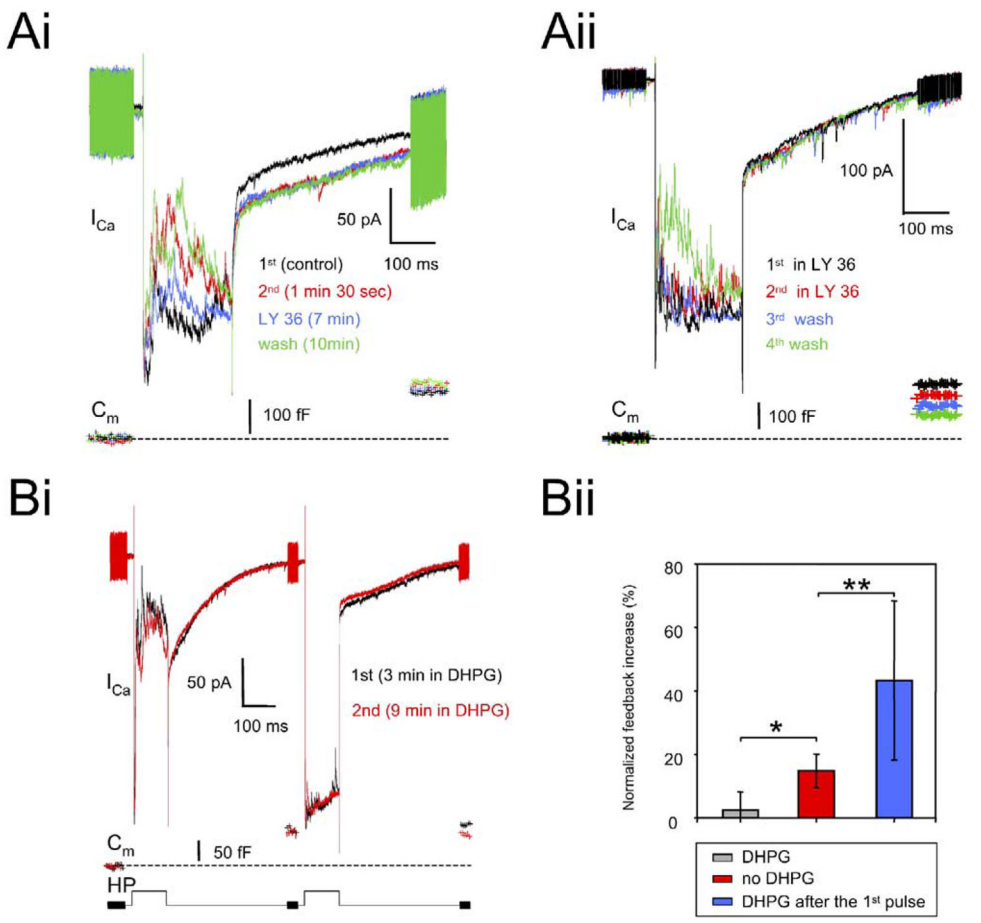

Figure 6. Synaptically Released Glutamate Evokes PSE via mGluR1 Activation

(Ai) PSE (compare black and red trace) could be reversibly eliminated by the use of the mGluR1 antagonist LY 367385 (100 μM). Several responses to a depolarizing pulse are shown superimposed (their timing after break-in is shown on the left); however, a nonpotentiated response obtained before the wash-out response (green trace) in not shown for clarity. Resting C_m of this terminal = 3.6 pF.

(Aii) If the retinal slices were bathed in LY 367385 (100 μM), the repeated depolarizations of the bipolar cell terminal did not lead to the enhancement of the feedback (first, 1 min and 46 s; second, 3 min and 26 s after break in). However, PSE took place if the blocker is washed away (compare blue and green traces, taken at 4 min and at 6 min and 26 s after break in, respectively). Interpulse intervals between consecutive traces: 90 s, 34 s, and 146 s, respectively. Resting C_m of this terminal = 4.3 pF.

(Bi) In the continuous presence of DHPG (100 μM), double pulses repeated from −60 to 0 mV for 100 ms (350 ms apart) did not evoke PSE. Note the great, presumably DHPG-enhanced reciprocal feedback for the first depolarizations in both black and red traces. Resting C_m of this terminal = 4.1 pF.

(Bii) Summary diagram of PSE magnitude in various DHPG conditions. Reciprocal feedback was evoked by depolarization of the bipolar cell terminal from −60 to 0 mV for 100 or 200 ms. PSE was quantified by the ΔQ_{Net} method in each condition. Continuous presence of DHPG (100 μM) occluded the PSE ("DHPG," gray bar, n = 6), whereas it enhanced PSE if applied between the two depolarizing steps ("DHPG after the 1st pulse," blue bar, n = 17). Both conditions were significantly different from the control PSE,

observed in the absence of DHPG (“no DHPG,” red bar, n = 24). *p < 0.001; **p < 0.0002, Student’s t test.

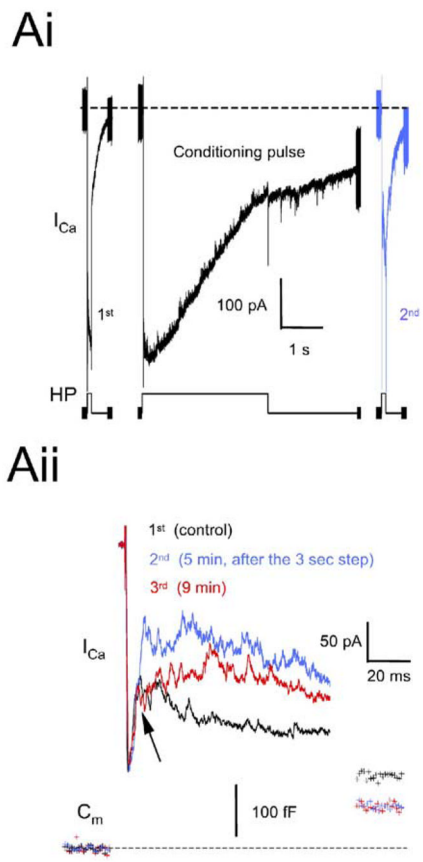

Figure 7. Poststimulus Enhancement Can Be Triggered by a More Physiological Depolarization of the Mb Bipolar Cell Terminal

(Ai) Bipolar cell terminals were depolarized from −60 to −20 mV for 100 ms twice with a 5 min interval (test pulses). In between, 2 min after the first test pulse, a 3 s long conditioning pulse (also from −60 to −20 mV) was applied. The resting C_m of this terminal was 4.0 pF. (Aii) Inset of (Ai). Overlaying the test pulses before (first) and after (second) the conditioning pulse revealed that potentiation of the reciprocal feedback is possible even at −20 mV by delivering a long conditioning pulse (−60 to −20 mV) between the test steps. The third test pulse 4 min later (approximately 7 min after the conditioning pulse) still evoked a larger reciprocal feedback response in this terminal (red trace), even after the rundown of the exocytosis (ΔC_m jump). Note that the first IPSC peaks occurred at ~3 ms (arrow). This is similar to what was measured following depolarizations to 0 mV (see Figure 1).

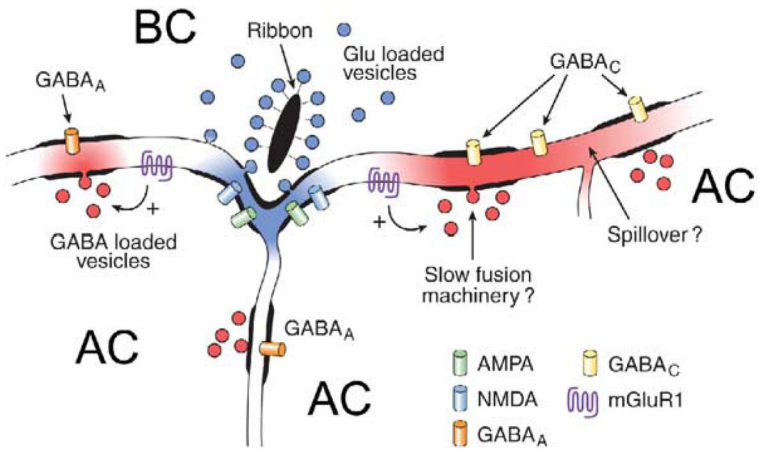

Figure 8. The Schematic Indicates the Different Cellular Components and Receptors that Are Involved in the Bipolar Cell (BC) to Amacrine Cell (AC) Reciprocal Synapse

The inhibitory GABAergic feedback can be augmented by activation of amacrine cell group I metabotropic glutamate receptors (mGluR1). The slow onset and long delay of the $GABA_C$ component of the inhibitory feedback may be intrinsic to the $GABA_C$ receptor or may be due to a slower synaptic vesicle fusion machinery or to GABA spillover activating extrasynaptic $GABA_C$ receptors.